Study on the formation and separation process of droplets in the medical piezoelectric atomization device induced by intra-hole fluctuation

Qiufeng Yan (yanqf@nuaa.edu.cn)
Nantong University https://orcid.org/0000-0003-1225-465X
Wanting Sun
Harbin Institute of Technology
Jianhui Zhang
Guangzhou University

Original Article

Keywords: CLSM, intra hole fluctuation, piezoelectric atomization, droplet distribution

Posted Date: July 21st, 2020

DOI: https://doi.org/10.21203/rs.3.rs-42852/v1

Study on the formation and separation process of droplets in the medical piezoelectric atomization device induced by intra-hole fluctuation

Qiufeng Yan [1*], Wanting Sun [2] Jianhui Zhang [3*]

[1] School of Electrical Engineering, Nantong University, Nantong 226019, P.R. China.

[2] School of Materials Science and Engineering, Harbin Institute of Technology, Harbin 150001, P.R. China.

[3] College of Mechanical and Electrical Engineering, Guangzhou University, Guangzhou 510006, P.R. China.

Abstract:

Oral inhalation of aerosolized drugs can be directly performed on the affected body organs including lesions of the throat, trachea as well as lungs. As compared to the other conventional therapies such as intravenous drip, intramuscular injection and external topical administration, this novel technique can greatly reduce the dosage and side effects of drugs. However, the traditional atomization devices always exhibit many drawbacks, such as wide spreading distribution of atomization particle size, the instability of transient atomization quantity and difficulties in precise energy control, which seriously restrict more extensive application of atomization inhalation therapy. The formation and separation process of droplets is a microphenomenon of atomization. Research on the droplet formation and separation process will help us to better understand the atomization mechanism. In present work, the Conservative Level Set Method (CLSM) is the first time to be applied on the simulation of the formation and separation of droplets in a medical piezoelectric atomization device induced by intra-hole fluctuation. The intra-hole fluctuation mechanism is analyzed in details, and also the expression of the volume change of the micro cone hole is evaluated. The control equation and simulation model of droplet formation and separation process has been well established by meshing the simulation model, and thereby the process of droplet formation and separation is simulated. The corresponding results demonstrate that the breaking time of droplets decreases with the increase of inlet velocity and liquid temperature, and increases with the increase of liquid concentration. Meanwhile, the volume of droplet decreases with the increase of

inlet velocity and liquid concentration, but increases with the increase of liquid temperature. The velocity of droplet is enhanced with the inlet velocity and liquid temperature rising, and reduced with the increase of liquid concentration. When the large side diameter of micro-cone hole is set as 79 μm, the breaking time of the droplet reaches a minimum value of 38.7 μs, whereas the volume and the velocity of droplet reaches a maximum value of 79.8 pL and 4.46m/s, respectively. This study reveals the atomization mechanism of the medical piezoelectric atomization device induced by intra-hole fluctuation from a micro perspective. It provides theoretical guidance for the design of medical piezoelectric atomization devices and contributes to the promotion of inhalation therapy in practical use.

Key words： CLSM, intra-hole fluctuation, piezoelectric atomization, droplet distribution

1. Introduction

The corona virus disease 2019 (COVID-19) has swept the whole world since the end of 2019, thus it caused serious economic losses and casualties [1]. Up to now, there is still a lack of specific drugs and vaccines precaution for COVID-19 virus. During the progress of fighting with the virus, the autoimmune ability of patients is particularly important. Working as one of the anti-virus treatment methods, Interferon-α is inhaled by atomization to enhance the autoimmune function by stimulating human immune cells [2]. Interferon-α can be fully dispersed into tiny droplets produced by the effect of atomization device, which directly acts on respiratory epithelial cells. It is noteworthy that the inhalation therapy contains a relative small dosage, avoiding and / or reducing the systemic medication so as to obviously weaken the toxic and side effects of the drugs. Simultaneously, inhalation therapy can relive the pain deriving from the injection and administration, since its operation is simple and convenient [3]. Consequently, in order to satisfy the needs of atomization therapy, many scholars have focused on the investigation of the medical atomization device.

In 2006, Vecellio [4] designed a kind of medical atomizer, which adopt

electroplating technology to process 6000 3-μm-diameter holes on the mesh plate. Under the excitation of the alternating current voltage, the piezoelectric transducer generates high-frequency vibrations to cause the atomization of the drug solution to form an aerosol. The respiratory system is directly connected with the lesion, achieving targeted and quantitative administration and reducing the side effects caused by systemic administration. In 2011, Lin et al. [5] used the laser ablation technology and electroforming technology to prepare a palladium-nickel alloy nozzle plate having a nozzle diameter of 5 μm. The nozzle plate prepared using this method is quite difficult and can be used at a frequency of 100 kHz. Studies have shown that the usage of this nozzle is effective for controlling the particle size of drug droplets during the progress of atomizing a drug solution. The average particle size of the atomized droplets is approximately 3 μm, which satisfies the requirement that the drug particles must be less than 4 μm when absorbed by the lungs. In 2012, Beck-Broichsitter et al. [6] proposed a vibrating-mesh-type nebulizer to atomize the prepared nanoparticle drugs. Experiments have confirmed that using nanoparticles to encapsulate sildenafil can maintain its stability and that atomizing the process does not affect the particle size, particle size distribution, or sildenafil content. In addition, Rottier [7], Lenney [8], Montgomery [9] et al. researchers have also worked on the inhalation therapy.

Both the atomization rate and particle size are expected to play a pronounced role in the inhalation therapy. Olseni [10] and Mitchell [11] et al. found that when the drug particles are not larger than 5 μm, they can enter the airway and lungs. Subsequently, they can be deposited on a lesion by gravity. It should be pointed out that the drug particles can be deposited on the lesion, so that the diameter of drug particles cannot be larger than 4 μm. Simultaneously, a constant atomization rate can make the treatment process of patients feel more comfortable.

In the process of atomization, the formation and separation of droplets is considered as a typical gas-liquid two-phase flow. It is difficult in tracing the free interface of gas-liquid two-phase flow. A Marker-And-Cell (MAC) method to track the position of free surface was developed by Harlow [12]. Subsequently, scholars

proposed some methods to solve these problems. For instance, Simplified-MAC (SMAC) [13], Arbitrary Boundary Method (SUMAC) [14], Stanford University Modified MAC (SUMMAC) [15], Tokyo University Modified Marker-And-Cell (TUMMAC) [16], Volume of Fluid (VOF), Level Set Method (LSM) [18].

VOF and LSM are regarded as two most commonly used free interface tracking approaches in recent reports. By comparison, LSM seems more popular used in interface tracking, because it can obtain the information of unit normal vector and curvature radius of interface, which overcomes the defect of VOF method that is difficult to simulate the necessary unit normal vector and curvature radius, [19-21]. Nevertheless, the traditional LSM also shows poor conservation easily resulting in mass loss, thus affecting the accurate positioning of the interface leads to an appearance of wrong results. In order to improve the conservation of mass, in the convective phase of the level set, several hybrid methods have been employed, for instance, combining LSM with VOF to obtain VOF-LSM [22]. However, this algorithm will increase the complexity of computation and waste the advantages of LSM. For simplification of the calculation process of VOF-LSM and promotion in the accuracy of LSM, Olsson et al. [23,24] proposed a CLSM approach on the basis of LSM. The key point of CLSM is to utilize a 0.5 horizontal plane working as the gas-liquid interface, which can successfully improve the calculation accuracy.

The formation and separation process of droplets is a micro phenomenon of atomization. Studies on droplet formation and separation process will help us to better understand the atomization mechanism. In this study, the CLSM is the first time to be conducted on the simulation of the formation and separation of droplets in a medical piezoelectric atomization device induced by intra-hole fluctuation. The intra-hole fluctuation mechanism is systematically analyzed, and the expression of the volume change of the micro cone hole is evaluated. The control equation and simulation model of droplet formation and separation process are established. Simultaneously, the process of droplet formation and separation is simulated. This study reveals the atomization mechanism of the medical piezoelectric atomization device induced by intra-hole fluctuations from a micro perspective . It is anticipated to provide some

theoretical guidance for the design of medical piezoelectric atomization devices and contribute to the promotion of inhalation therapy in practical use.

2. Construction of atomization experiment platform

Figure 1 shows the atomization experiment platform of the medical piezoelectric atomization device induced by intra-hole fluctuation. Insulating clamps were used to mount the atomizer piece and fixed by a machine vise, which was placed on the lifting platform. The height of the atomizer piece was adjusted by the lifting platform to make sure the atomizer piece only touch the cotton stick (there was no gap or applied force between the sheet atomizer piece only touched the cotton stick (there was no gap or applied force between the sheet and the swab). The cotton stick was placed in a container filled with liquid. Because of the capillary force action, the liquid was flowed from the container to the atomizer pieceas indicated by the the blue arrow. Under the excitation of AC signal, the inner wall of the micro cone hole will fluctuate and cause the change of the volume of the micro cone hole. Simultaneously, because of the existence of the difference between the positive and negative flow resistance of the micro cone hole, it will produce a pumping effect [25] to remove the liquid from the cotton stick to the external environment, thereby producing the atomization phenomenon. Figure 2 illustrates the photograph of the atomization experiment of the medical piezoelectric atomization device induced by intra-hole fluctuation.

Figure 3 shows the structure and parameters of the atomizer piece. It can be seen from Fig.3 that the piezoelectric vibrator is composed of dispenser and piezoelectric ceramic ring. The outer diameter, inner diameter, and thickness of the piezoelectric ceramic ring are set as values of 15.96mm, 7.69mm and 0.63mm, respectively, while the diameter and thickness of the dispenser are 15.96 mm and 0.05 mm respectively. The taper holes with diameter of 740 μm were machined in the center area of the piezoelectric atomizer.

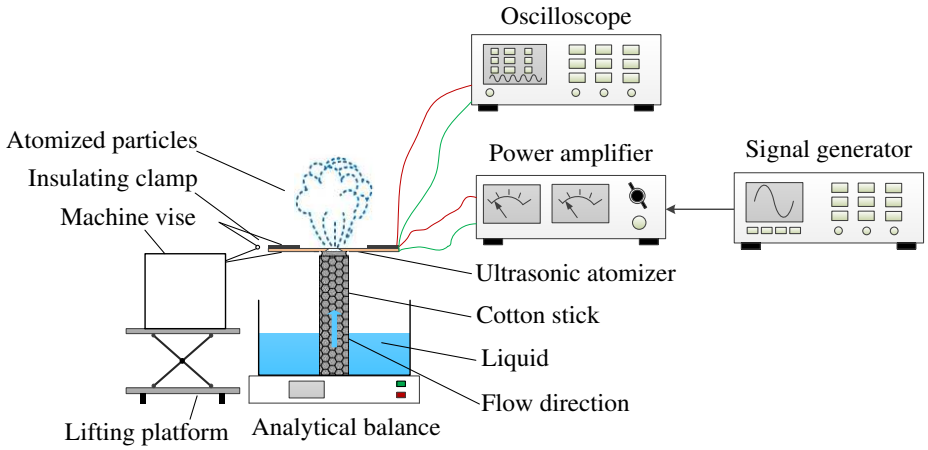

Figure 1 Atomization experiment platform of the medical piezoelectric atomization device induced by intra-hole fluctuations

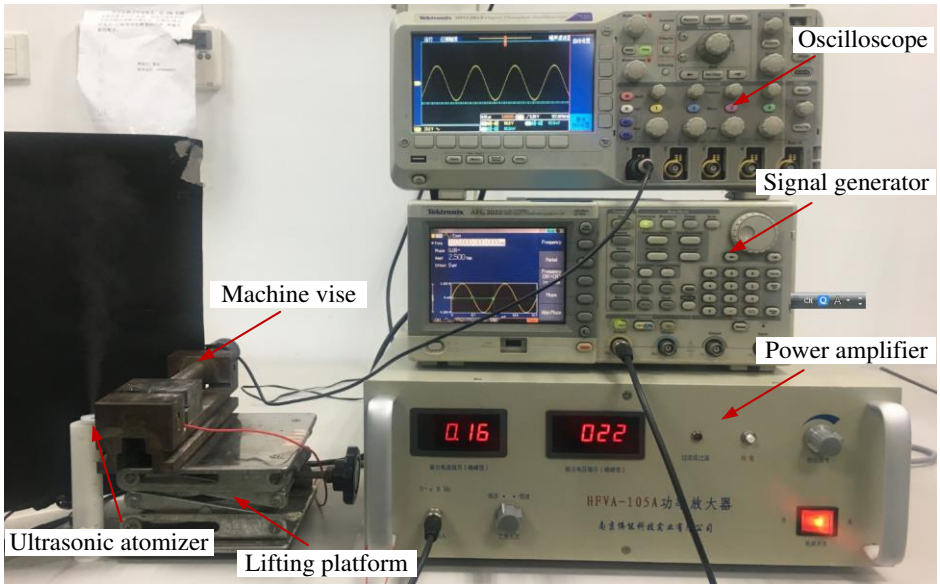

Figure 2 Photograph of the atomization experiment of the medical piezoelectric atomization device induced by intra-hole fluctuations.

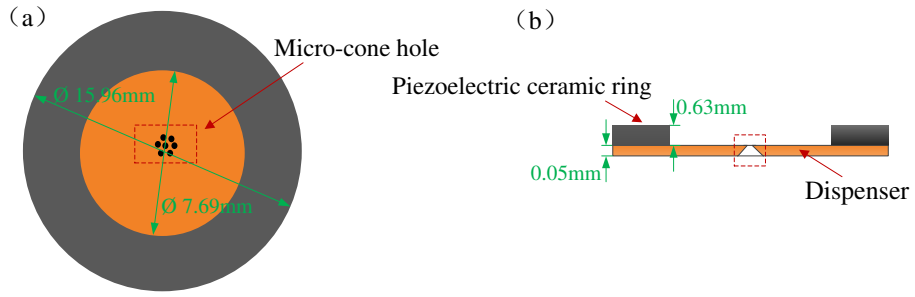

（a）Overhead view　　（b）Elevation view

Figure 3 The schematic diagram showing the structure and parameters of the atomizer piece used in this work

3. Theoretical analysis of the intra-hole fluctuation mechanism in the medical piezoelectric atomization device

Figure 4 shows the deformation process of micro-cone hole in a cycle. Under the excitation of AC voltage, the piezoelectric ceramic ring can generate alternating compressive and tensile forces on the dispenser to drive the vibration of the dispenser. As the micro cone hole is located on the substrate, the inner wall of the micro-cone hole can fluctuate with the vibration of the dispenser causing a change in volume, and then the pressure change inside the micro-cone hole can produce atomization. This cycle continues as long as the piezoelectric ceramic ring is remained to deliver the required stimulation.

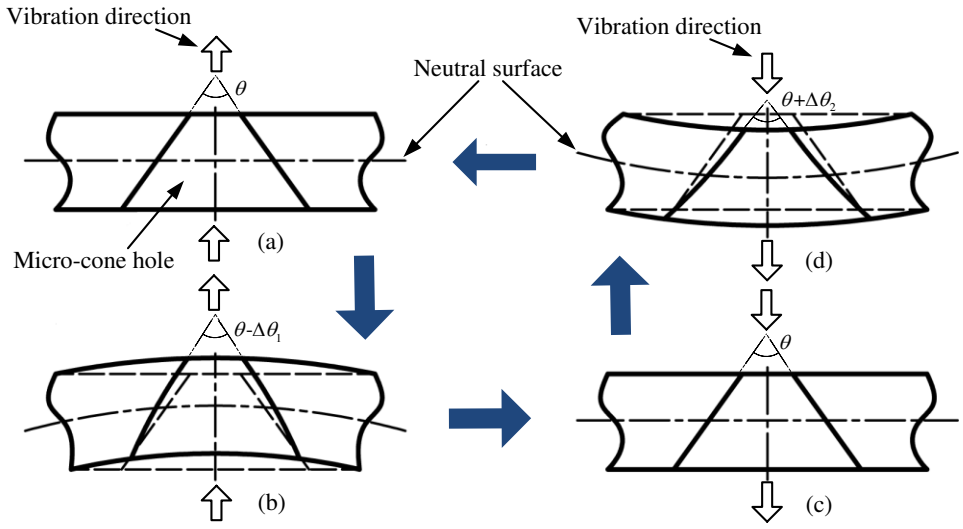

Figure 4 The schematic diagram of deformation process of micro-cone hole in a cycle

The coordinate system is built by Kirchhoff hypothesis, the neutral surface of the dispenser is distributed with the *xy* plane and the z axial is perpendicular to it, as shown in Fig. 5(a). According to the Kirchhoff hypothesis, the velocity and amplitude of the upper and lower vibrations of the dispenser are symmetric with respect to the equilibrium position. In order to better illustrate the deformation of the apertures, the *xz* plane is shown in Fig. 5(b). Simultaneously, there is no movement of the dispenser neutral surface in *x* and *y* directions. Any straight line which is vertical to the neutral surface before its deformation is still vertical to the elastic and flexible plane after its deformation. The length of the line remains the same during this progress .

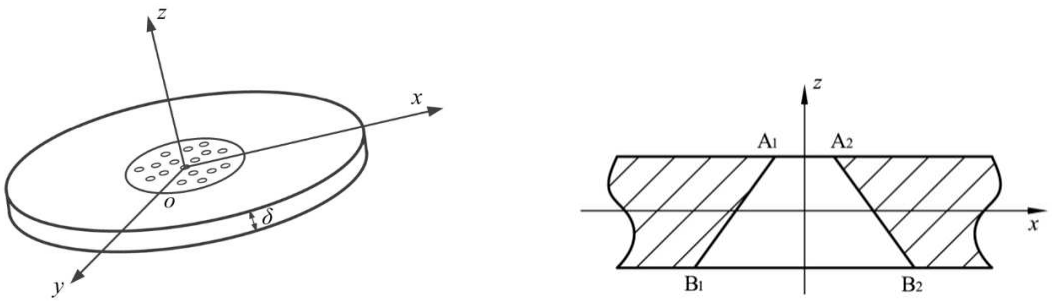

（a）Coordinate system of the dispenser （b）Profile of a micro-cone hole

Figure 5 Schematic diagram of coordinate settings of the dispenser

If the neutral surface is set as a plane of $q(x,y)$, the movement from N to N' on the dispenser as given in Fig.6, where MN line is perpendicular to the xy plane, and M'N' line is perpendicular to the surface $q(x,y)$.

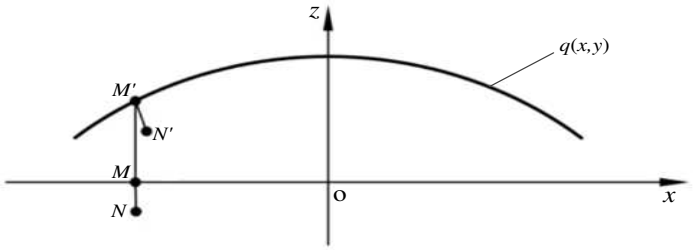

Figure 6 Deformation process of a point in the dispenser

After the occurrence of deformation, the point of M(x_0, y_0, 0) is changed to another position as M' [x_0, y_0, $q(x_0, y_0)$] . According to Kirchhoff hypothesis, Eq. (1) is the normal format at M' on the neutral surface after the deformation:

$$\begin{cases} x = x_0 - q_x\left[z - q(x_0, y_0)\right] \\ y = y_0 - q_y\left[z - q(x_0, y_0)\right] \end{cases} \tag{1}$$

Where q_x and q_y refer to the partial derivatives of $q(x,y)$ at x_0 and y_0, respectively.

According to Kirchhoff hypothesis, after calculation the equation of $|\mathrm{MN}| = |\mathrm{M'N'}| = |z_0|$ can be achieved.

$$\left[(x_0 - x_0^{'})^2 + (y_0 - y_0^{'})^2 + (q(x_0, y_0) - z_0^{'})^2\right]^{\frac{1}{2}} = |z_0| \tag{2}$$

The coordinate of N' is calculated by Eq. (1) and Eq. (2), and the result is shown as Eq. (3).

$$(x_0 - bq_x, y_0 - bq_y, b + q) \tag{3}$$

Where $b = z_0 \Big/ \left(1+q_x^2+q_y^2\right)^{\frac{1}{2}}$.

The surface equation for a micro-cone hole is written by Eq. (4).

$$\left(x^2+y^2\right)^{\frac{1}{2}} = -\tan\left(\frac{\alpha}{2}\right)\cdot z + r_m \tag{4}$$

Where α is the half angle of micro-cone hole, and r_m is the diameter of the circle on its neutral surface.

In order to estimate the entire volume changes of the micro-cone hole, it's necessary to calculate the volume changes of its micro unit.

It is assumed that a micro unit at point $E_1(x, y, z)$, its dimensions are Δx, Δy and Δz, respectively. The result of its volume before the deformation is calculated by Eq. (5).

$$\Delta V_{\mathrm{f}} = \Delta x \cdot \Delta y \cdot \Delta z \tag{5}$$

With the help of second order Taylor expansion of the function at point $E_1(x, y, z)$, and the ignorance of the infinitesimal of high order, the vectors of the three sides of the micro unit at the top after deformation can be obtained using the Eq. (6)-Eq. (8).

$$\mathbf{v}_x = \left[\Delta x - bq_{xx}\Delta x - b_x q_x \Delta x, -\left(bq_{yx}\Delta x + b_x q_y \Delta x\right), b_x \Delta x + q_x \Delta x\right] \tag{6}$$

$$\mathbf{v}_y = \left[-\left(bq_{xy}\Delta y + b_y q_x \Delta y\right), \Delta y - bq_{yy}\Delta y - b_y q_y \Delta y, b_y \Delta y + q_y \Delta y\right] \tag{7}$$

$$\mathbf{v}_z = \left[-b_z q_x \Delta z, -b_z q_y \Delta z, b_z \Delta z\right] \tag{8}$$

As mentioned above, the dispenser is vibrating symmetrically to the original neutral surface. For simplified the calculation, it is reasonable to assume that the function of the neutral surface is $q(x, y)$ when the dispenser reaches the highest position during vibrations, and the function of the neutral surface is $-q(x, y)$ when the dispenser reaches the lowest position during vibrations.

The volumes of a micro-cone hole can be evaluated by Eq. (9) when the dispenser reaches the highest positions during vibrations.

$$V_u = \iiint_{\Omega}\left[s^{\frac{1}{2}} + z^2\left(q_{xx}q_{yy} - q_{xy}^2\right)s^{-\frac{3}{2}} + z\begin{pmatrix}-q_{yy} - q_{xx} - q_y^2 q_{xx} + \\ 2q_x q_y q_{xy} - q_x^2 q_{yy}\end{pmatrix}s^{-1}\right]dV \tag{9}$$

Where $s = 1 + q_x^2 + q_y^2$.

The volumes of a micro-cone hole can be calculated by Eq. (10) when the dispenser reaches the lowest positions during vibrations.

$$V_d = \iiint_{\Omega} \begin{bmatrix} s^{\frac{1}{2}} + z^2 \left(q_{xx} q_{yy} - q_{xy}^2 \right) s^{-\frac{3}{2}} + \\ z\left(q_{yy} + q_{xx} + q_y^2 q_{xx} - 2 q_x q_y q_{xy} + q_x^2 q_{yy} \right) s^{-1} \end{bmatrix} dV \qquad (10)$$

Where $s = 1 + q_x^2 + q_y^2$.

The maximum change (Eq. (11)) of the micro-cone hole volume during vibrations can be confirmed by the subtraction of Eq. (10) and Eq. (9).

$$\Delta V_K = \iiint_{\Omega} \left[2z\left(q_{yy} + q_{xx} + q_y^2 q_{xx} - 2 q_x q_y q_{xy} + q_x^2 q_{yy} \right) s^{-1} \right] dV \qquad (11)$$

Where $s = 1 + q_x^2 + q_y^2$.

According to the calculation above, the volume change of the micro-cone hole is directly proportional to the driving voltage during a vibration cycle. The volume change caused by the fluctuation of the inner wall of the micro cone hole will provide the driving force for atomization of the atomizer.

4. Numerical simulation of the formation and separation process of droplets

Actually, during the process of atomization, the formation and separation of droplets belongs to a typical gas-liquid two-phase flow. It seems quite difficulty in tracing of the free interface of the gas-liquid two-phase flow due to their complexity.

4.1 Establishment of governing equations

In this study, the CLSM approach is used to describe the characters of liquid interface. In this method, the 0.5 level is used as the interface of liquid and air. The CLSM can present a high calculation accuracy to distinguish and divide the liquid and air. The mass and momentum transfer of fluid are expressed by the incompressible N-S equation (including surface tension). Because of the velocity of liquid and air is lower than that of sound, they can be treated as incompressible fluid. Accordingly, the N-S equation and continuity equation can be obtained as followings.

$$\begin{cases} (\rho\vec{u})_t + \nabla\cdot(\rho\vec{u}\vec{u}) = -\nabla p + \dfrac{1}{\mathrm{Re}}\nabla\left(\mu\left(\nabla\vec{u} + (\nabla\vec{u})^T\right)\right) + \dfrac{\rho}{Fr^2}\vec{e}_g + \dfrac{1}{We}\vec{F}_{sv} \\ \nabla\cdot\vec{u} = 0 \\ \Phi_t + \nabla\cdot(\Phi\vec{u}) = 0 \end{cases} \tag{12}$$

Where $\mathrm{Re} = \rho_{ref}u_{ref}l_{ref} \big/ \mu_{ref}$, $Fr = u_{ref}\cdot\left(l_{ref}\cdot g\right)^{-\frac{1}{2}}$, $We = \dfrac{\rho_{ref}u_{ref}^2 l_{ref}}{\sigma}$, and ρ_{ref}、μ_{ref}、l_{ref} and u_{ref} are constants representing the density, viscosity, lengthand velocit y of the liquid respectively And σ is the surface tension coefficient.

For CLSM, the 0.5 level is used as the interface of liquid and air, in which the factor of 1 is used for liquid, and the factor of 0 is used for air. At the interface between liquid and air, the parameter of Φ transition from 0 to 1 is smooth. Therefore, the convection equation of the level set function after reinitialization can be rewritten as follows:

$$\frac{\partial\Phi}{\partial t} + \vec{u}\cdot\nabla\Phi + \gamma\left[\left(\nabla\cdot\left(\Phi(1-\Phi)\frac{\nabla\Phi}{|\nabla\Phi|}\right)\right) - \varepsilon\nabla\cdot\nabla\Phi\right] = 0 \tag{13}$$

In this case, ε is determined by the thickness of the interface between liquid and air, where $\varepsilon = hc/2$, hc represents the size of a typical grid of droplets passing through the region. γ is determined by the amount of reinitialization, that is, the stability of the level set function Φ, which is mainly affected by the interface velocity of liquid and air.

Surface tension play a dominant role in role in the process of droplet spraying. In the process of simulation, the surface tension should be taken into account to get the droplet velocity and size.

The continuous surface tension model is adopted under this condition.

$$F_{sv} = \sigma\delta(\Phi)\kappa(\Phi)\mathbf{n} \tag{14}$$

Where $\mathbf{n}, \sigma, \kappa(\Phi), \delta(\Phi)$ are direction vector of interface, surface tension coefficient, curvature, Dirac delta function of interface, respectively.

In order to improve the calculation accuracy of surface tension, the surface tension is further modified by the weak solution form of momentum equation (Eq. (15)).

$$F_{sv} = \nabla \cdot \left[\sigma \left(\mathbf{I} - \left(\mathbf{n}\mathbf{n}^{T} \right) \right) \delta(\Phi) \right] \quad (15)$$

Where $\mathbf{I}$ is defined as an identity matrix.

In order to simplify the calculation, Dirac delta function is approximated as Eq. (16).

$$\delta(\Phi) = 6\left|\Phi(1-\Phi)\right|\left|\nabla\Phi\right| \quad (16)$$

4.2 Simulation model

Fig. 7 (a) shows the geometric outline of the liquid gas interface containing the air and the liquid chamber. In Fig. 7 (a), l_1 is the radius of the liquid storage chamber, l_2 is the thickness of the liquid storage chamber, l_3 is the length of the conical nozzle, l_4 is the length of the tip of the conical nozzle, l_5 is the radius of the tip of the conical nozzle, l_6 is the length of the air chamber, l_7 is the outlet radius, and the related characteristic dimensions of the geometric contour are listed in Table 1. In order to precisely analyze the cross section between liquid and air, adaptive mesh generation is used, that is, in the simulation process, with the interface moving, the mesh will be updated automatically. Fig. 7 (b) shows the mesh generation diagram, the model is divided into numerous triangular meshes. Because the model is set as an axisymmetric image and only half one side is taken as a representation for caculation, and then the other one side model can be obtained through the mapping principle.

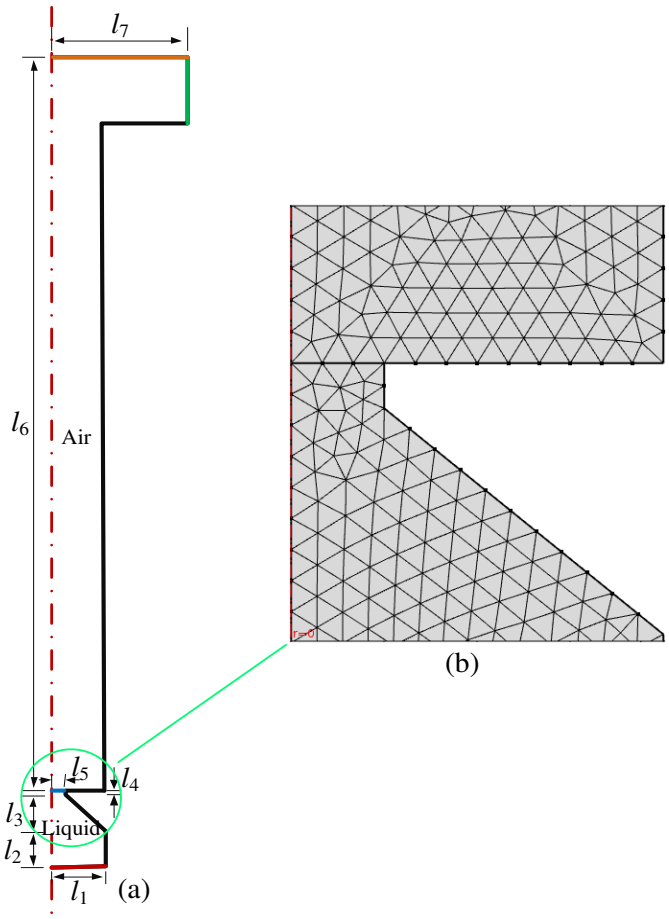

Figure 7 The applied simulation model and mesh partition used in CLSM method.

Table 1 Feature size of simulation model

Liquid chamber					Air chamber	
l_1 (mm)	l_2 (mm)	l_3 (mm)	l_4 (mm)	l_5 (mm)	l_6 (mm)	l_7 (mm)
0.08	0.05	0.05	0.01	0.02	1	0.2

In this study, the atomization process of atomizer is also simulated by COMSOL. Water at the temperature is selected as the liquid part, and the surrounding medium is air. For the corresponding calculation of gas-liquid two-phase flow, the fluid region covers the water and air, and their physical properties are required to be fixed before the calculation. Table 2 shows the physical properties of liquid materials, including the density of liquid materials, the dynamic viscosity of liquid materials, and the surface tension of liquid materials, where the surface tension of air is set to the value

of 0.

Table 2 Physical properties of liquid materials

Medium	Density (kg/m^3)	Dynamic viscosity ($N.s/m^2$)	Surface tension (N/m)
Water	997.07	8.934×10^{-4}	0.072
Air	1.225	1.789×10^{-5}	

In Figure 7 (a), the red line denotes the inlet, the green line represents the outlet, the black line represents the wall, and the blue line represents the interface between gas and liquid. Additionally, the water liquid below the interface is indicated as blue line, and air is above the interface, and all the wall surfaces are supposed with no sliding. The target (brown part) is set as "wetted wall" condition with a contact angle of $\pi/2$. The outlet is set to a constant pressure of 1 atmosphere. By applying an inlet velocity $v(r)$ as the vibration velocity of the piezoelectric vibrator, the instantaneous velocity in z direction is: $v(r,t)=\sin(wt).v(r)$, the unit of t is s, w is frequency. When a sinusoidal signal is applied, the water fills the entire conical nozzle.

5. Results and discussion

5.1 Process of droplet formation

In this study, the research object of the atomized droplet is pure water and its physical properties are listed in Table 2. The process of droplet formation is simulated, and the changes of velocity and pressure in the process of droplet formation are discussed. in this case, the entrance boundary condition is set as a sine function with the maximum speed of 0.35 m/s, and the droplet spray process is obtained as seen in Fig.8. The process can be divided into several important stages in the droplet spray process: elongation, necking, fracture, formation of satellite droplet, fusion of satellite droplet and main droplet, droplet formation and other stages.

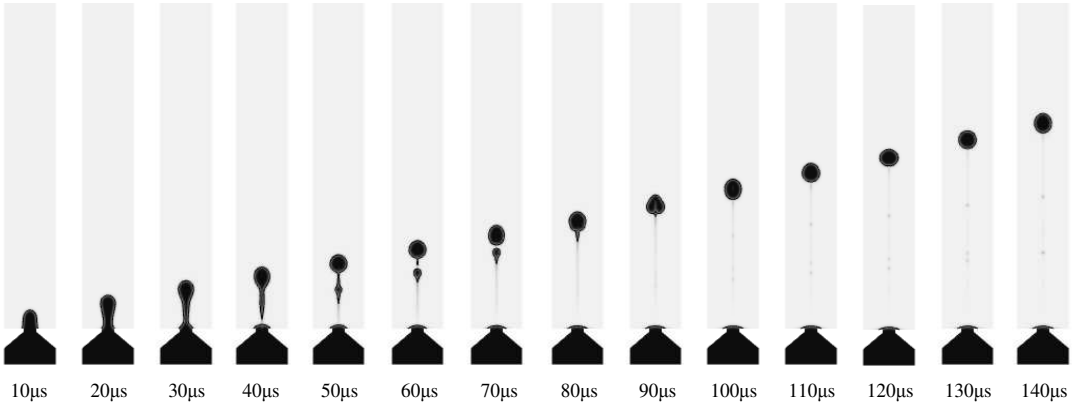

Figure 8 Process of droplet formation

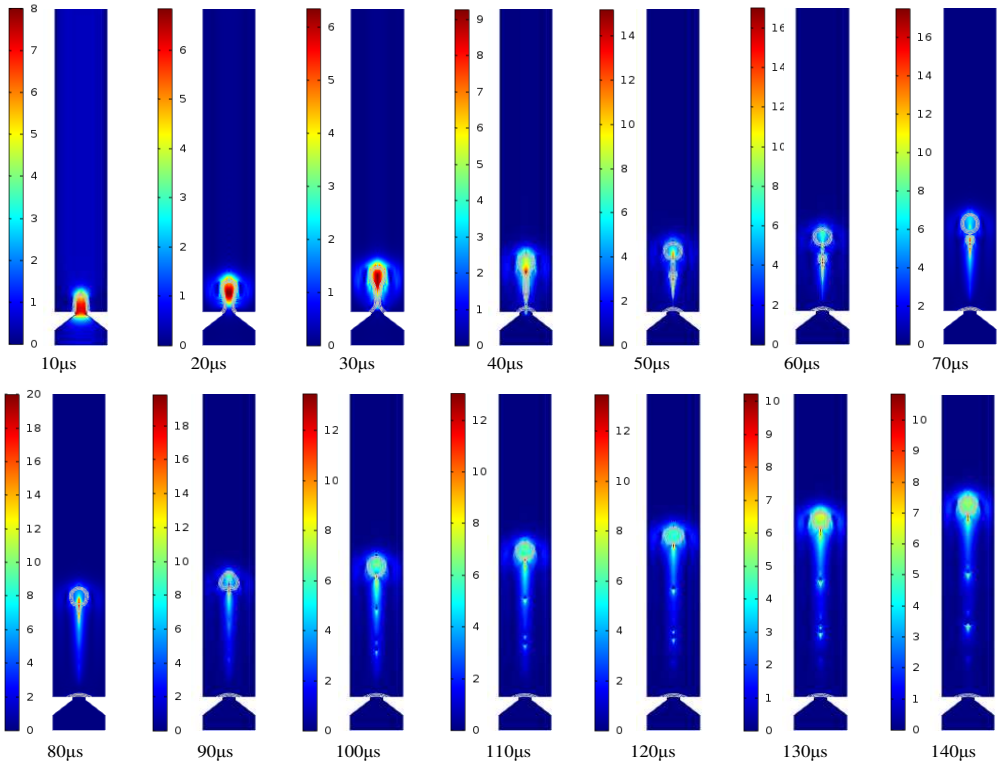

Figure 9 Velocity nephogram of the process of droplet formation

At the initial stage, due to the positive pressure inside the micro cone hole, the liquid will gradually flow out to form a liquid column. After a period of time, a “tongue like” bulge will be produced. Under the action of surface tension, the front end of the liquid column will shrink into a circle. It can be seen from the velocity nephogram of the process of droplet formation shown in Figure 9 that the velocity of the fluid in the central region of the micro cone hole is higher than that of the nearby fluid. It can be explained by the fact that the fluid near the wall of the micro cone hole is much more significantly affected by the wall adhesion force. Simultaneously, it is

found from the pressure nephogram of the process of droplet formation shown in Figure 10 that the internal pressure of the droplet is greater than the external pressure, and the difference in the pressure can provide power for the movement of the droplet. At the duration of 21 μs, the liquid column will stop extending, and necking phenomenon will appear under the combined action of negative pressure, inertia, pipe wall friction and surface tension in the micro cone hole. At this stage, through the velocity nephogram, it is apparent that the velocity of the front end of the droplet is larger than that of the back end, so that the liquid column will be gradually elongated. The front part and backward part of the liquid column is named as the main droplet and tail droplet, respectively. The velocity difference between the main droplet and the tail droplet will keep the liquid column growth?. At 38.8 μs, the liquid column will break completely and spray out. According to the velocity nephogram above, the front-end velocity of droplet is greater than that of back-end droplet. As time prolongs to 52.3 μs, the main droplet and tail droplet will be disconnected to form satellite droplet. Subsequently, the main droplet will form a stable circle under the combined action of the main air force and surface tension. After the formation of the spherical droplet, the air resistance of the droplet will rise up and the droplet speed will slow down. Simultaneously, it can be seen from the pressure nephogram that the pressure inside the satellite droplet is greater than that of the main droplet, which will provide more power for the movement of the satellite droplet, so that the satellite droplet will gradually fuse with the main droplet ahead. At the last stage of 71.7 μs, the satellite droplet will fuse with the main droplet.

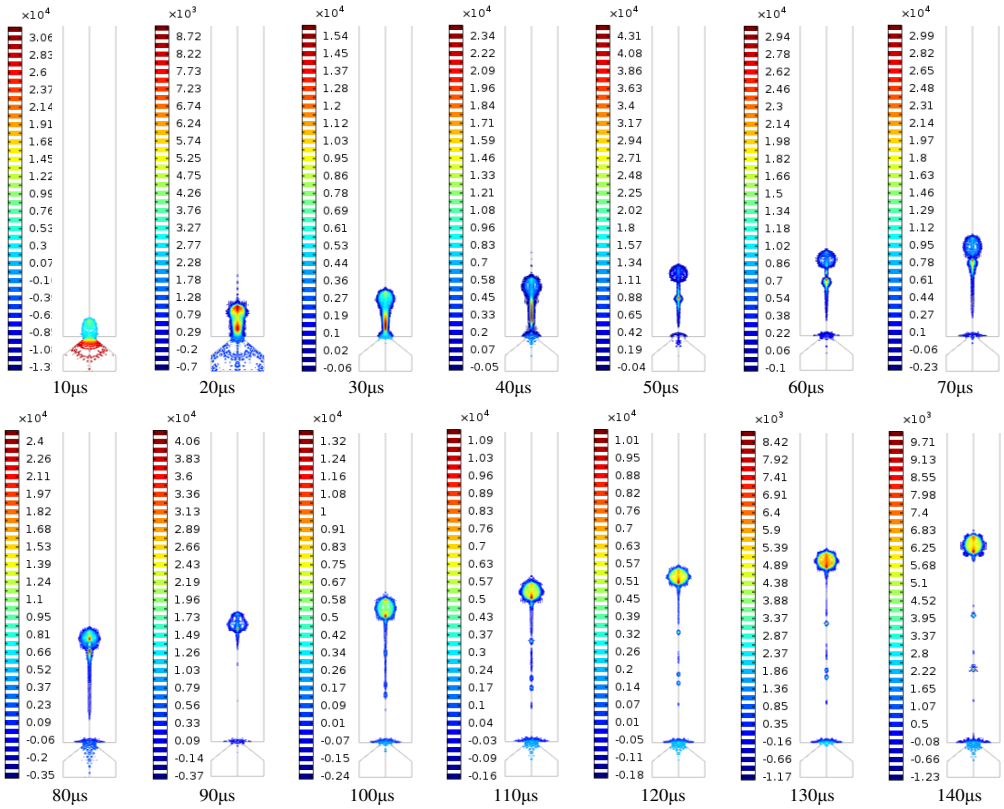

Figure 10 Pressure nephogram of the process of droplet formation

5.2 Effects of inlet velocity on droplet formation

Figure 11 shows the relationships among breaking time of droplet, volume of droplet, velocity of droplet and inlet velocity. The simulation results show that when pure water is selected as the liquid at the temperature of 25℃, the volume and velocity of droplet almost linearly increase with inlet velocity increasing, while the breaking time of the droplet decreases. However, when the inlet velocity is greater, this shows that the deformation of the piezoelectric vibrator is larger, and the energy applied to the liquid is also large. With the increase of the applied energy, the droplet is easier to get rid of the bondage of the surface tension and spray into the air, so the breaking time of droplet is decreased. Similarly, with the increase of energy, the droplet will also obtain greater initial kinetic energy, and its velocity will be faster. With the increase of deformation, the volume of liquid at the injection point will increase in one cycle, so the volume of droplet will be also enhanced.

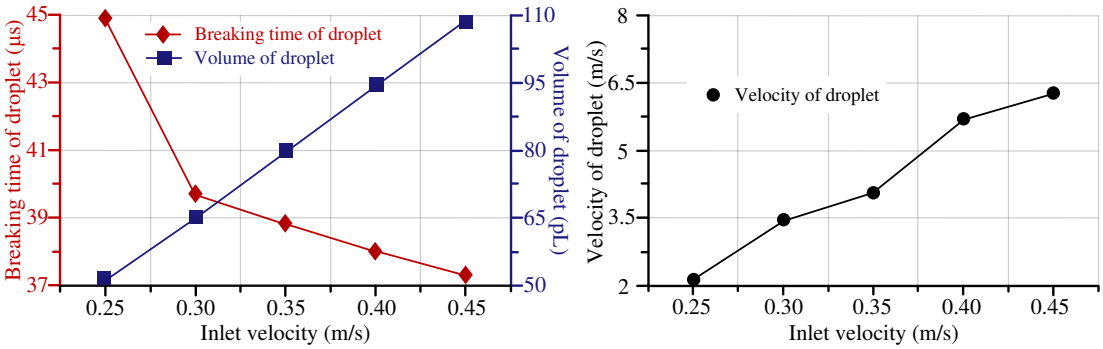

Figure 11 The relationship among breaking time of droplet, volume of droplet, velocity of droplet and inlet velocity

5.3 Effects of liquid temperature on droplet formation

Figure 12 shows the relationship among breaking time of droplet, volume of droplet, velocity of droplet and liquid temperature. The simulation results show that when the inlet velocity is 0.35 m/s and the liquid choose pure water, with the liquid temperature rising, the breaking time of liquid is prolonged, the volume of droplet decreases, and the velocity of droplet increases, but the overall change trend is not obvious. This phenomenon can be ascribed to the following factors: (i) with the increase of liquid temperature, the viscosity and surface tension of the liquid will decrease. (ii) The energy consumed to overcome the viscous resistance will be reduced, and the velocity of the droplet will be increased. (iii) With the decrease of viscosity, the resistance of droplet formation will be decreased, and the breaking time of droplet will be decreased, and the volume of droplet will be increased.

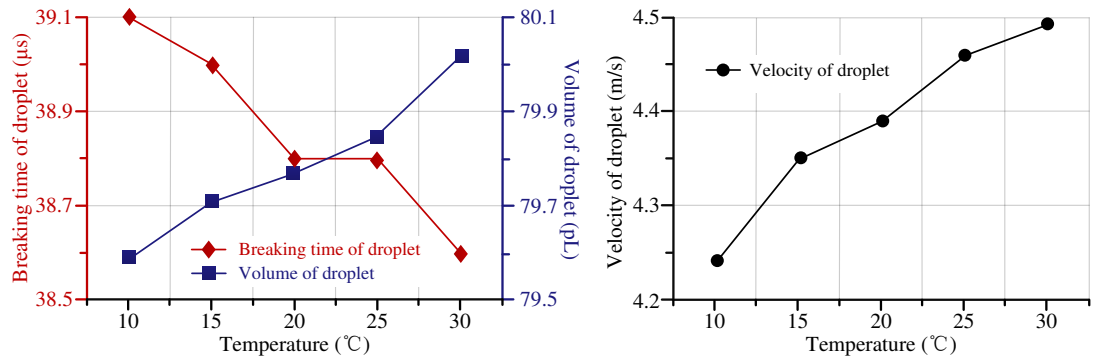

Figure 12 The relationship among breaking time of droplet, volume of droplet, velocity of droplet and liquid temperature

5.4 Effect of liquid concentration on droplet formation

Figure 13 shows the relationship among breaking time of droplet, volume of droplet, velocity of droplet and liquid concentration. It can be concluded from the simulation results that when the inlet velocity is 0.35 m/s and the liquid temperature is 25℃, the breaking time and volume of droplet increase, and the velocity of droplet decreases, but the overall change trend is not obvious. The reason for the above phenomenon can be described by the fact that with the increase of the concentration of NaCl solution, the viscosity and surface tension of the liquid increased. The energy consumed to overcome the viscous resistance increases and the velocity of the droplet decreases. With the increase of the droplet viscosity, the resistance of droplet formation increased, the breaking time of the droplet increases and the volume decreases.

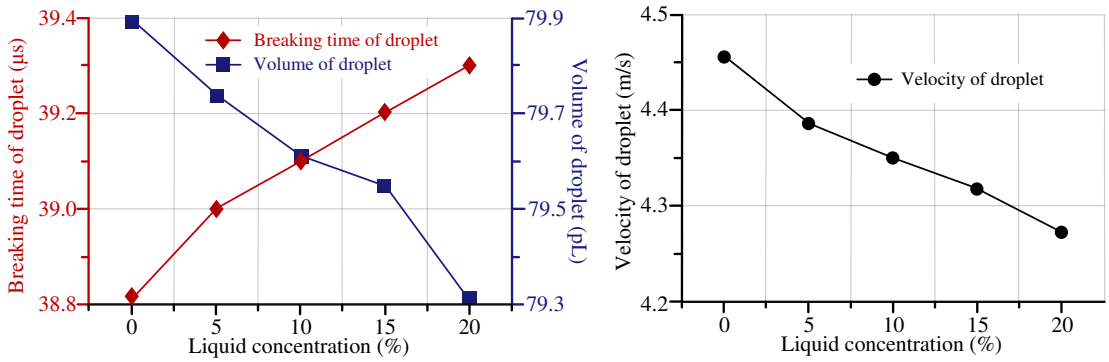

Figure 13 The relationship among breaking time of droplet, volume of droplet, velocity of droplet and liquid concentration

5.5 Effects of micro-cone hole angle on droplet formation

In order to verify the influences of the cone angle on the droplet formation process, the small side diameter of micro-cone hole is set as 10μm. By changing the large side diameter of micro-cone hole, the taper hole with different angles can be obtained. Figure 14 shows the relationship among breaking time of droplet, volume of droplet, velocity of droplet and large side diameter of micro-cone hole. The simulation data show that when the liquid is pure water, the liquid temperature is 25℃, the inlet velocity is 0.35 m/s, the breaking time of the droplet exhibits a minimal value of 38.7 μs when the large side diameter of the micro nozzle is 79 μm, the volume of the droplet is 79.8pL, the velocity of the droplet reach at a maximum

value of 4.46m/s. The reason for the above phenomenon is that the micro-cone hole participates in the formation of droplets. Owing to the variation in the large side diameter of the micro-cone hole, the flow resistance is also changing constantly, which affects the formation of the droplet.

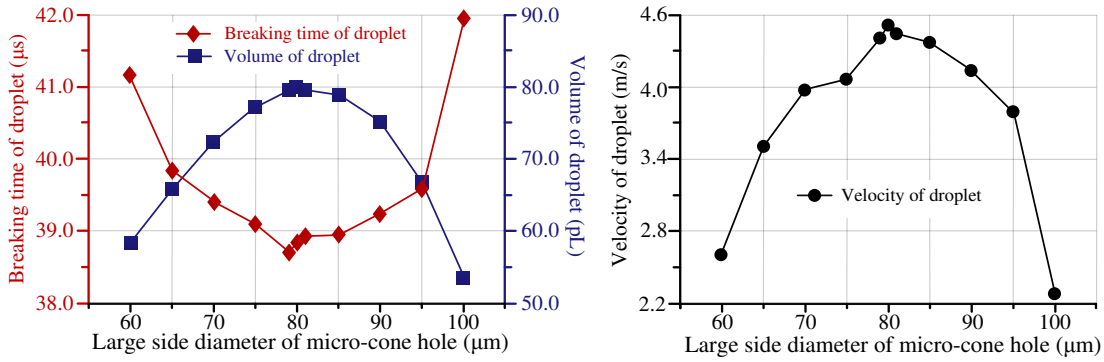

Figure 14 The relationship among breaking time of droplet, volume of droplet, velocity of droplet and large side diameter of micro-cone hole

6. Conclusion

In this study, the separation and formation process of droplets in a medical piezoelectric atomization device induced by intra-hole fluctuation were investigated. The related atomization mechanisms were revealed from the micro point of view. It is anticipated to provide theoretical guidance for designing a king of novelmedical piezoelectric atomization device. The conclusions of this research are summarized as follows:

(1) In order to solve the problem that the level set method usually cause mass loss during droplet separation, which affects the accurate positioning of the interface. CLSM is applied to the simulation of the formation and separation of droplets in atomizer. The simulation model of liquid-gas interface was established by COMSOL, and the mesh division, material property setting and boundary condition setting are carried out. Simultaneously, the droplet separation process of atomizer was simulated by COMSOL.

(2) The simulation results show that the velocity of the fluid in the central region of the micro cone hole is greater than that of the nearby fluid, the internal pressure of the droplet is greater than the external pressure, and the difference of the pressure can provide power for the movement of the droplet. Ultimately, the effects of inlet

velocity, liquid temperature, liquid concentration and the angle of micro-cone hole on the droplet separation process were discussed.

(3) According to the simulation data, it is clearthat the breaking time of droplet decreases with the increase of the inlet velocity and liquid temperature, but increases with the increase of the concentration of NaCl solution, and the breaking time of droplet is shorted to a value of 38.7 μs when the diameter of the large side diameter of the micro-cone hole is 79 μm. The volume of droplet decrease with the increase of the inlet velocity and the concentration of NaCl solution, increases with the increase of liquid temperature. At the same situation, the volume of droplet is largest value of 79.8 pL. The velocity of droplet increases with the increase of the inlet velocity and liquid temperature, decreases with the increase of the concentration of NaCl solution, and thus the velocity is the maximum value of 4.46m/s.

Acknowledgements

The authors would like to acknowledge the financial support from the Guangdong Basic and Applied Basic Research Foundation.

Authors' contributions

Jianhui Zhang and Qiufeng Yan was in charge of the whole trial; Qiufeng Yan wrote the manuscript; Wanting Sun revised the English of this manuscript. All authors read and approved the final manuscript.

Authors' Information

Qiufeng Yan, born in 1988, is currently a lecturer at School of Electrical Engineering, Nantong University, Nantong 226019, China. He received his PhD from Nanjing University of Aeronautics and Astronautics (NUAA), China, in 2019. His research interests include piezoelectric driving technology and ultrasonic atomization devices.

Wanting Sun, born in 1987, is currently works as a research associate at School of Materials Science and Engineering, Harbin Institute of Technology, Harbin, 150001, China. She received her PhD degree from Harbin Institute of Technology (HIT), China, in 2018. Her research interests mainly focus on the design of light-weighted

alloys with high performance used in industrial engineering.

Jianhui Zhang, born in 1963, is currently a professor at College of Mechanical and Electrical Engineering, Guangzhou University, Guangzhou 510006, China. He received his PhD from Yamagata University, Japan, in 2001. His research interests include chain transmission technology, piezoelectric driving technology and ultrasonic atomization devices.

Funding

Supported by Guangdong Basic and Applied Basic Research Foundation (2019B1515120017).

Availability of Data and Materials

The datasets supporting the conclusions of this article are included within the article.

Competing Interests

The authors declare no competing financial interests.

References

[1] Shah, Bhumi; Modi, Palmi; Sagar, Sneha R. In silico studies on therapeutic agents for COVID-19: Drug repurposing approach [J]. Life sciences, 2020, 252: 117652.

[2] Sadler A J, Williams B R. Interferon-inducible antiviral effectors [J]. Nature reviews, Immunology, 2008, 8(7):559-568.

[3] Ali M. Engineered aerosol medicine and drug delivery methods for optimal respiratory therapy [J]. Respiratory Care, 2014, 59(10): 1608-1610.

[4] Vecellio L. The mesh nebuliser: a recent technical innovation for aerosol delivery [J]. Breathe, 2006, 2(3): 252-260.

[5] Lin C Y, Meng H C, Fu C. An ultrasonic aersol therapy nebulizer using electroformed palladium-nickel alloy nozzle plates [J]. Sensors and Actuators A: Physical, 2011, 169: 187-193.

[6] Beck-Broichsitter M, Kleimann P, Gessler T. Nebulization performance of biodegradable sildenafil-loaded nanoparticles using the Aeroneb® Pro: Formulation aspects and nanoparticle stability to nebulization [J]. International journal of

pharmaceutics, 2012, 422(1): 398-408.

[7] Rottier B L, van Erp C J P, Sluyter T S. Changes in performance of the ParieFlow® rapid and Pari LC Plus™ during 6 months use by CF patients [J]. Journal of aerosol medicine and pulmonary drug delivery, 2009, 22(3): 263-269.

[8] Lenney W, Edenborough F, Kho P. Lung deposition of inhaled tobramycin with eFlow rapid/LC Plus jet nebuliser in healthy and cystic fibrosis subjects [J]. Journal of Cystic Fibrosis, 2011, 10(1): 9-14.

[9] Montgomery A B, Vallance S, Abuan T. A randomized double-blind placebo-controlled dose-escalation Phase 1 study of aerosolized amikacin and fosfomycin delivered via the PARI investigational eFlow inline nebulizer system in mechanically ventilated patients [J]. Journal of aerosol medicine and pulmonary drug delivery, 2014, 27(6): 441-448.

[10] Olseni L, Palmer J, Wollmer P. Quantitative evaluation of aerosol deposition pattern in the lung in patients with chronic bronchitis [J]. Physiological Measurement, 1994, 1(5): 41-48.

[11] Mitchell J P, Nagel M W. Particle size analysis of aerosols from medicinalinhalers [J], Powder&Particle, 2004: 32-65.

[12] Harlow F H, Welch J E. Numerical calculation of time-dependent viscous incompressible flow [J]. Physics of fluids, 1965, 8: 2182-2189.

[13] Amsden A A, Harlow F H. A simplified MAC technique for incompressible fluid calculation [J]. Journal of Computational Physics, 1970, 6: 322-325.

[14] Viecelli J A. A computing method for incompressible flows bounded by moving walls [J]. Journal of Computational Physics, 1971, 8: 119-143.

[15] Chan K C, Stree R L. A computer study of finite amplitude water wave [J]. Journal of Computational Physics, 1970, 6: 68-94.

[16] Hino T, Miyata H, Kajitani H. A numerical method for nonlinear shallow water (first report) [C]. Proceedings of Japanese Society of Architecture, 1983, 153: 1-12.

[17] Nichols B D, Hirt C W. SOLA-VOF: A solution algorithm for transient fluid flow with multiple free-boundaries [R]. Los Alamos Scientific Laboratory report, 1980, LA-8355.

[18] Osher S, Sethian J A. Fronts propagating with curvature dependent speed: Algorithms based on Hamilton-Jacobi formulations [J]. Journal of Computational Physics, 1988, 79(1): 12-49.

[19] Houhou N, Thiran J, Bresson X. Fast texture segmentation based on semi-local region descriptor and active contour [J]. Numerical Mathematics-theory Methods and Applications, 2009, 2(4): 445-468.

[20] Lowry N, Mangoubi R, Desai M, et al. Texton-based segmentation and classification of human embryonic stem cell colonies using multi-stage Bayesian level sets [A]. IEEE International Symposium on Biomedical Imaging (ISBI) [C]. IEEE, 2012, 194-197.

[21] Zong H M, Liu H, Ma Q P, et al. VCUT level set method for topology optimization of functionally graded cellular structures [J]. Computer Methods in Applied Mechanics and Engineering, 2019, 354(1): 487-505.

[22] Jiang Y, Li H, Chen C, et al. Calculation and verification of formula for the range of sprinklers based on jet breakup length [J]. International Journal of Agricultural & Biological Engineering, 2018, 11(1): 49-57.

[23] Olsson E, Kreiss G. A conservative level set method for two phase flow [J]. Journal of Computational Physics, 2005, 201: 225-246.

[24] Olsson E, Kreiss G, Zahedi S. A conservative level set method for two phase flow Ⅱ [J]. Journal of Computational Physics, 2007, 225: 785-807.

Figures

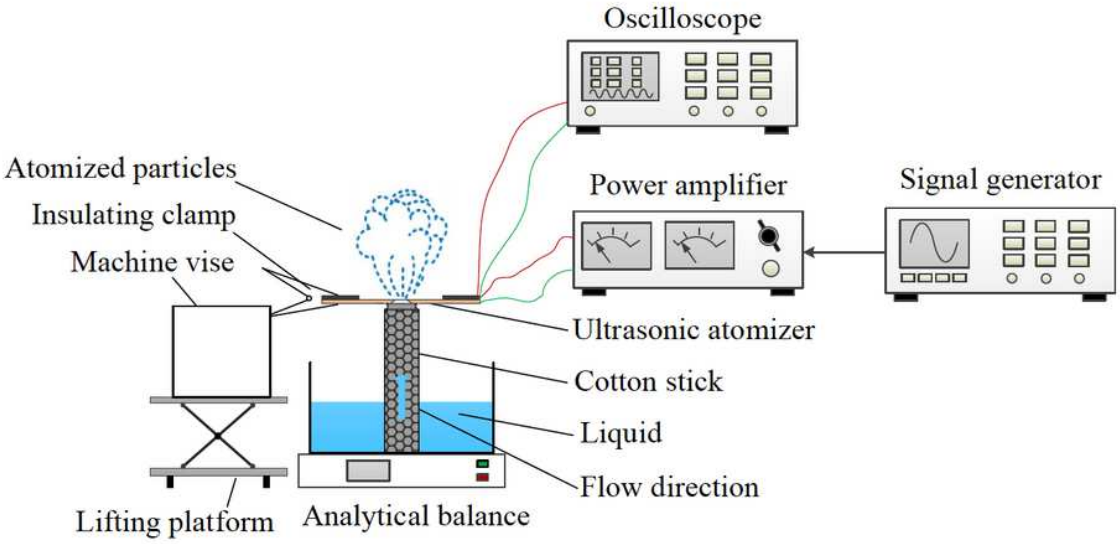

Figure 1

Atomization experiment platform of the medical piezoelectric atomization device induced by intra-hole fluctuations

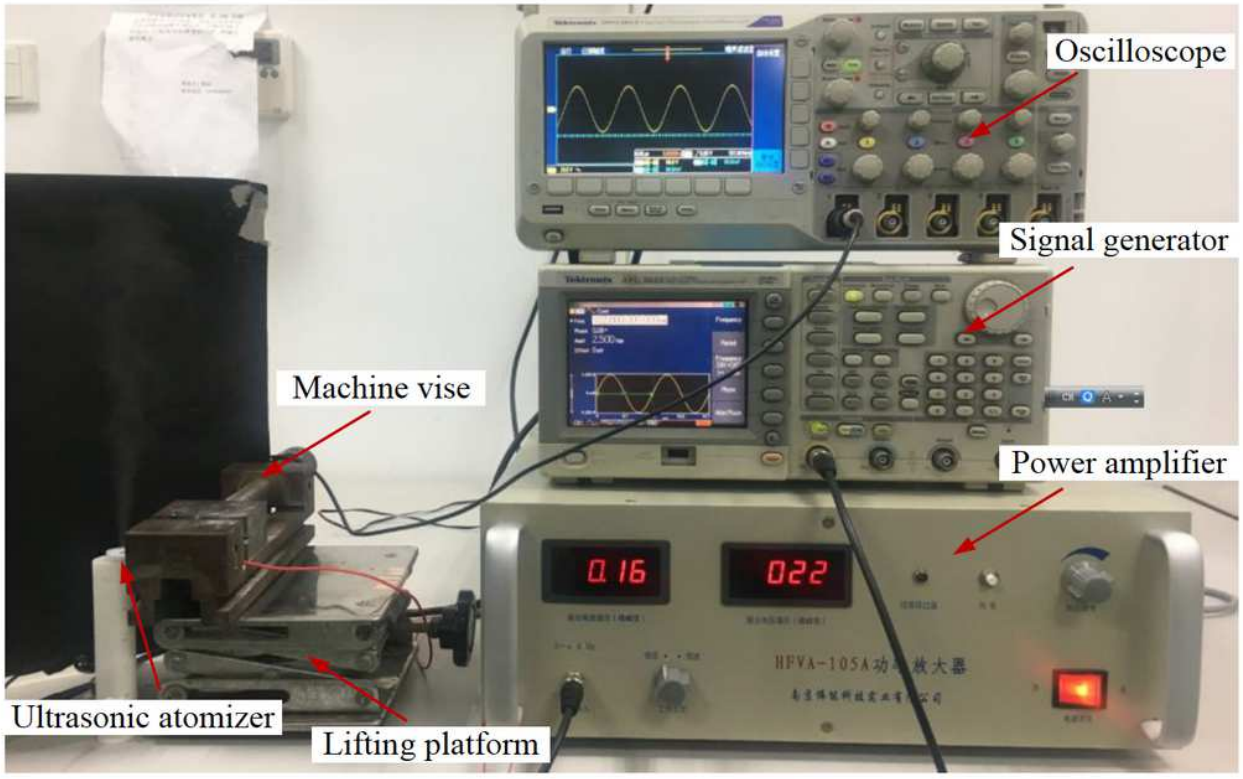

Figure 2

Photograph of the atomization experiment of the medical piezoelectric atomization device induced by intra-hole fluctuations.

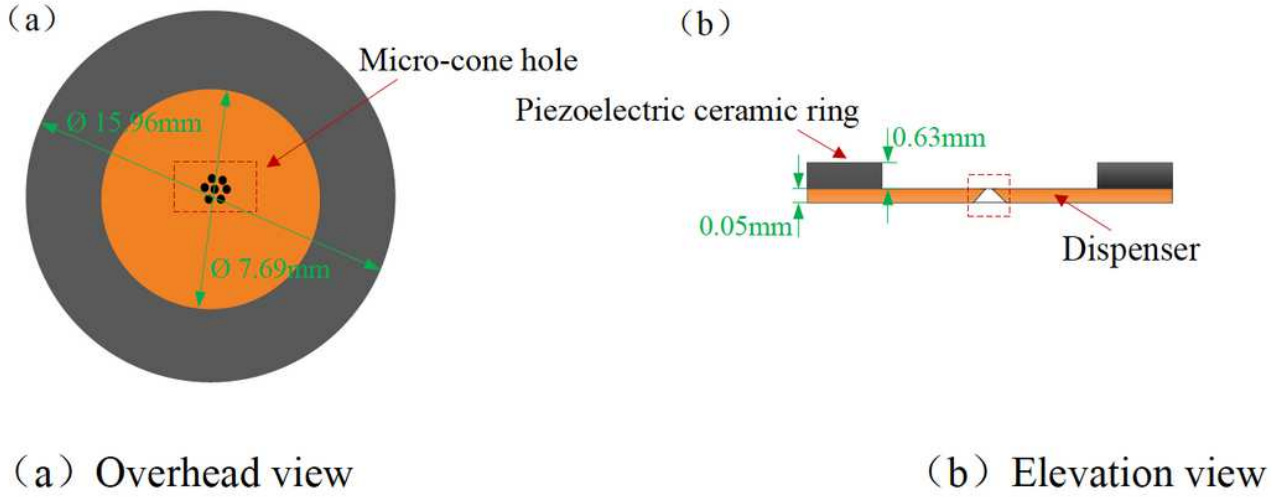

Figure 3

The schematic diagram showing the structure and parameters of the atomizer piece used in this work

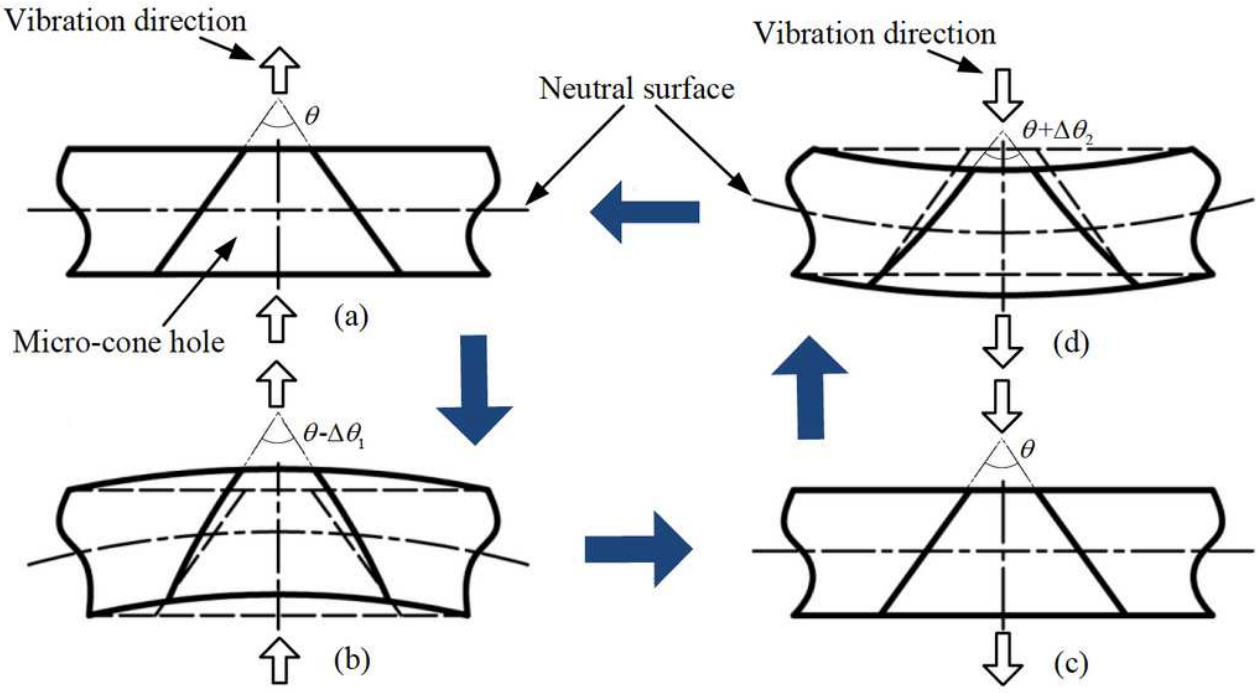

Figure 4

The schematic diagram of deformation process of micro-cone hole in a cycle

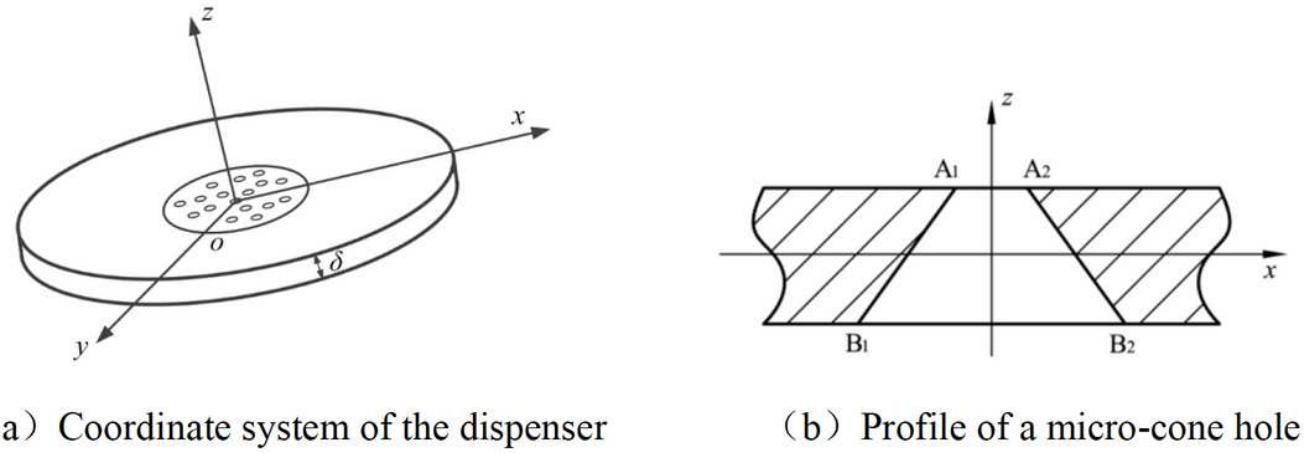

（a）Coordinate system of the dispenser　　（b）Profile of a micro-cone hole

Figure 5

Schematic diagram of coordinate settings of the dispenser

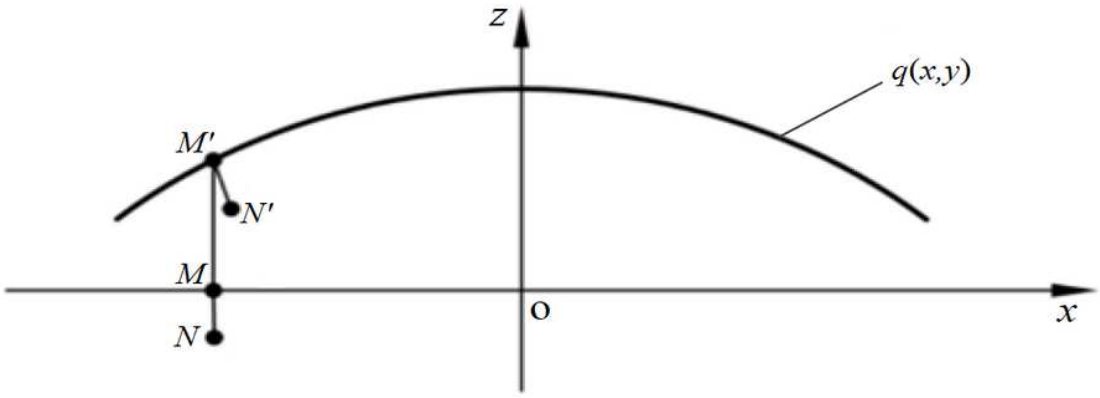

Figure 6

Deformation process of a point in the dispenser

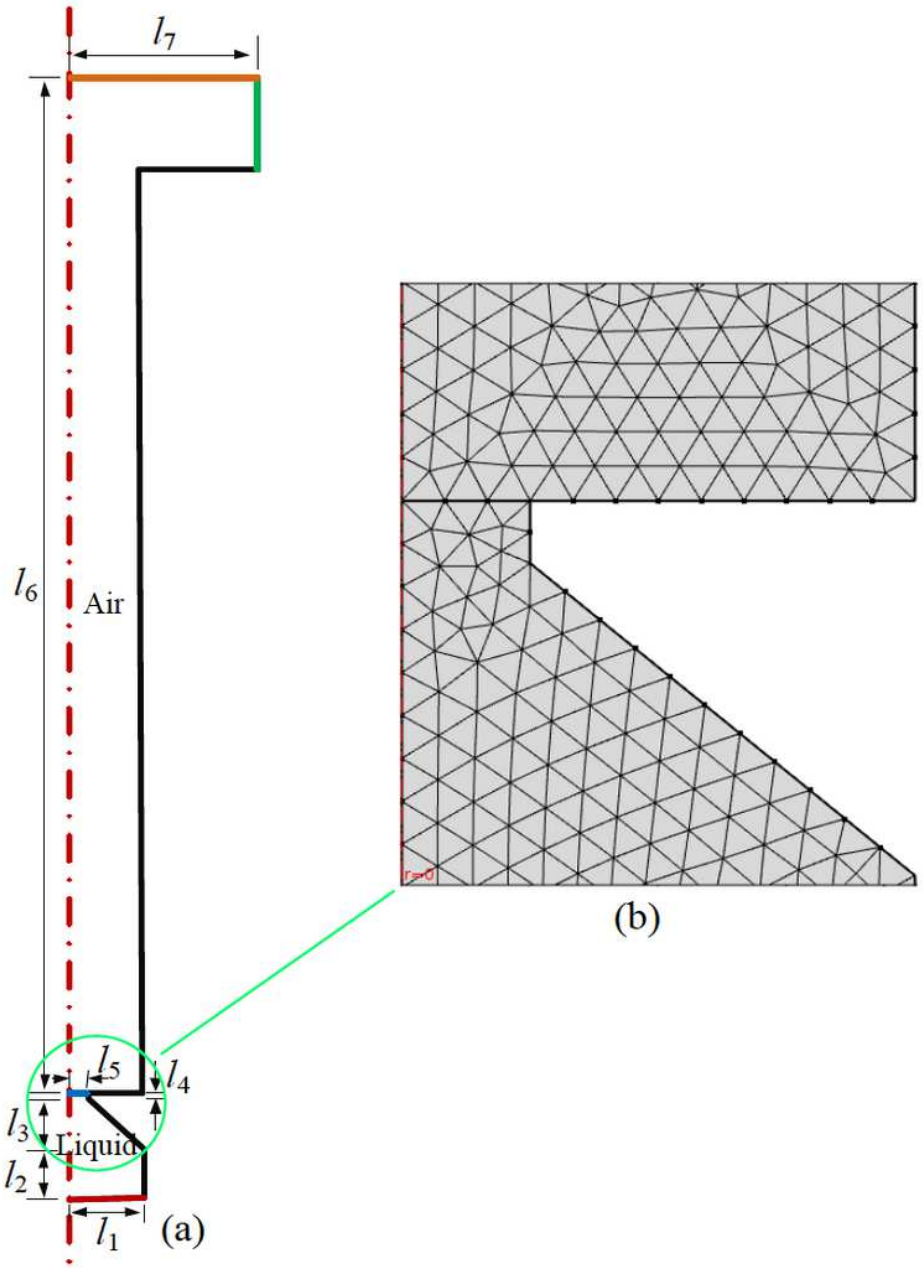

Figure 7

The applied simulation model and mesh partition used in CLSM method.

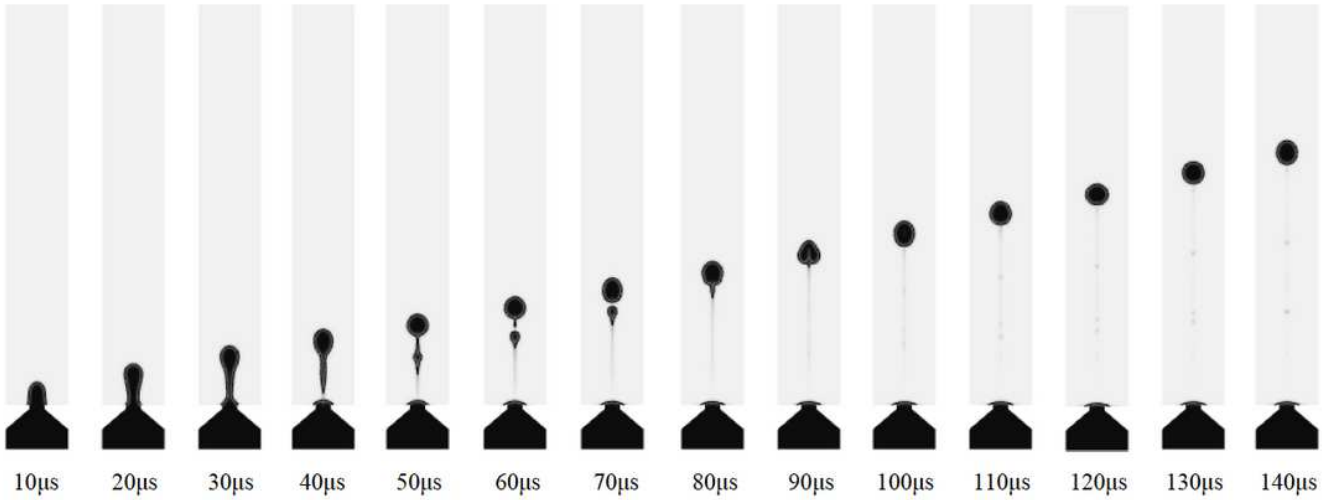

Figure 8

Process of droplet formation

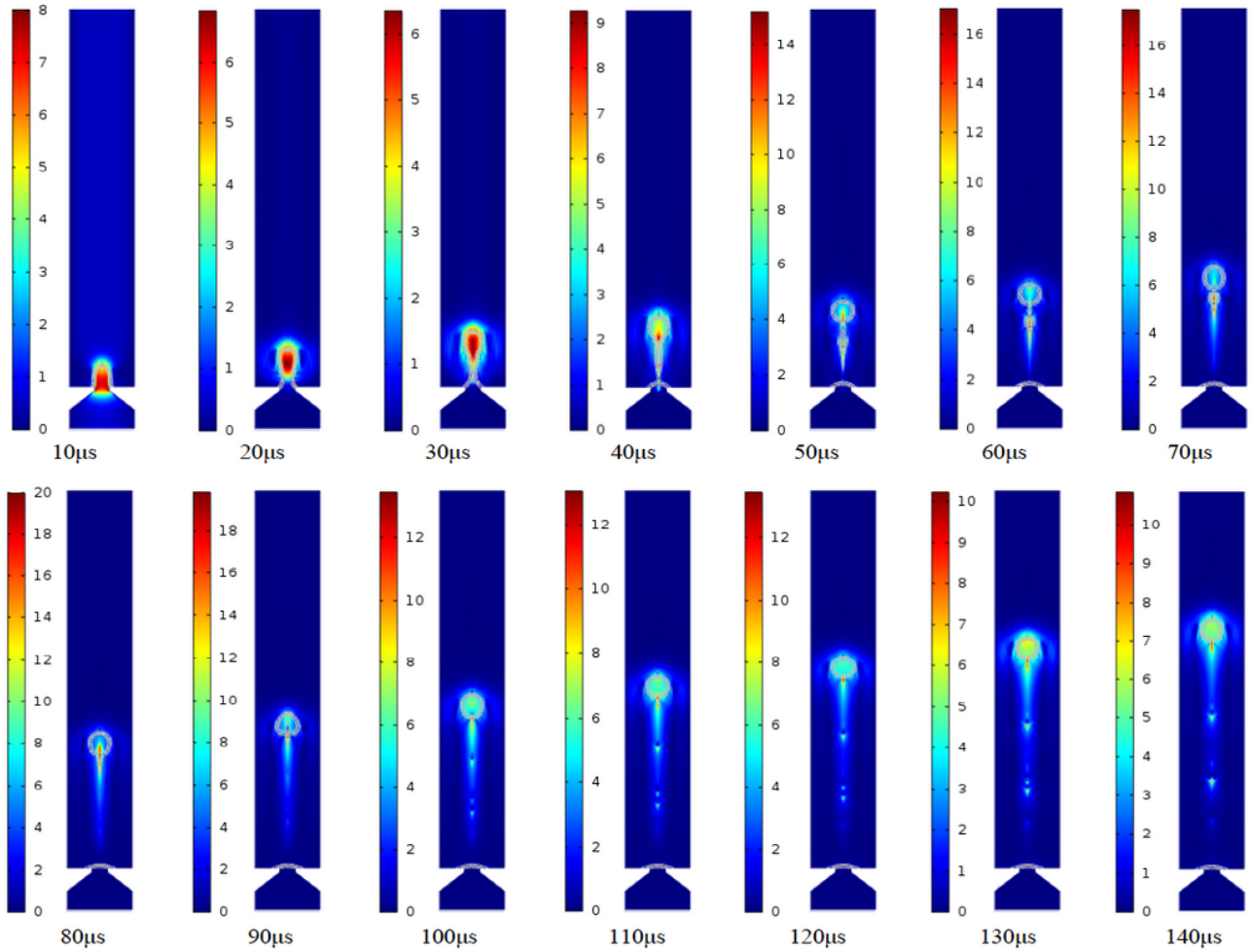

Figure 9

Velocity nephogram of the process of droplet formation

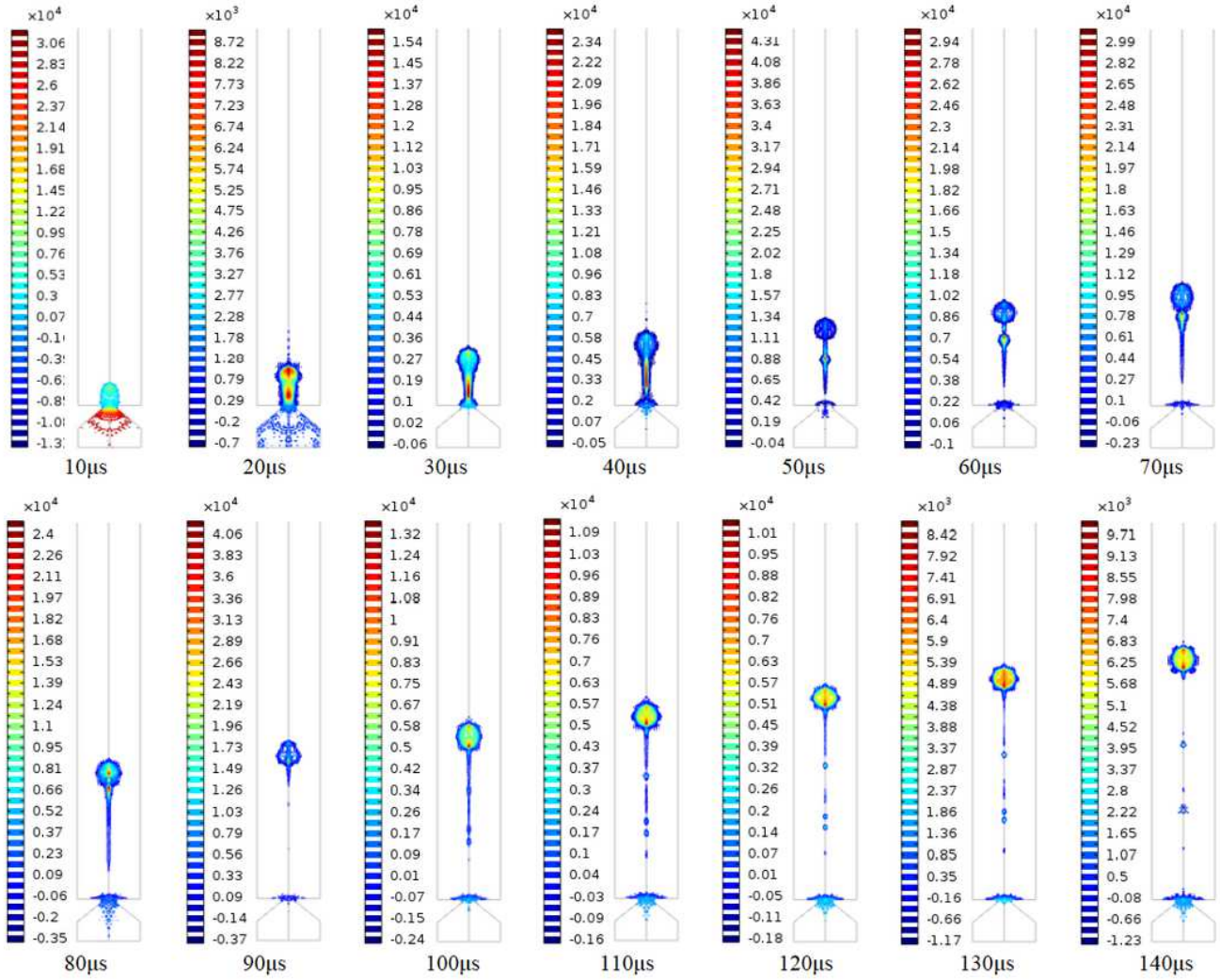

Figure 10

Pressure nephogram of the process of droplet formation

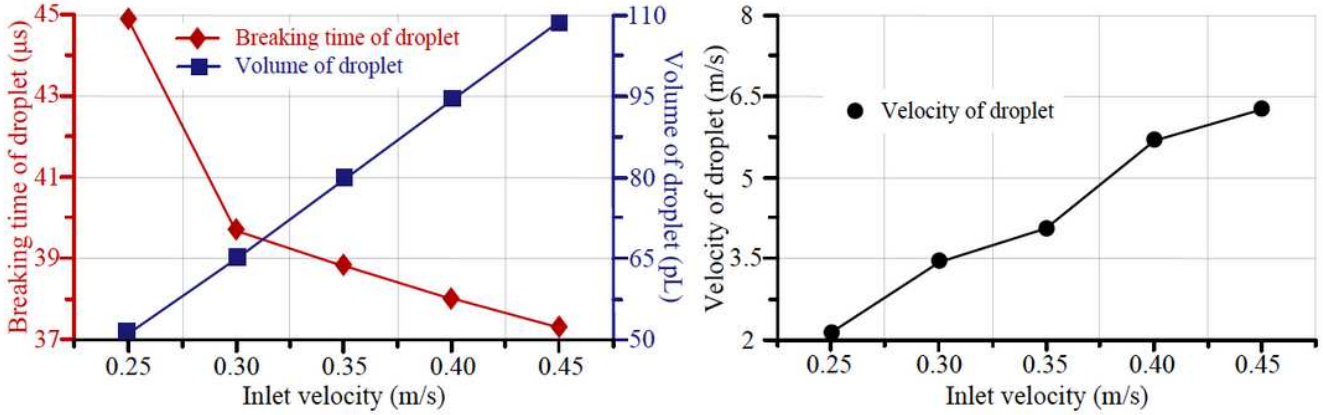

Figure 11

The relationship among breaking time of droplet, volume of droplet, velocity of droplet and inlet velocity

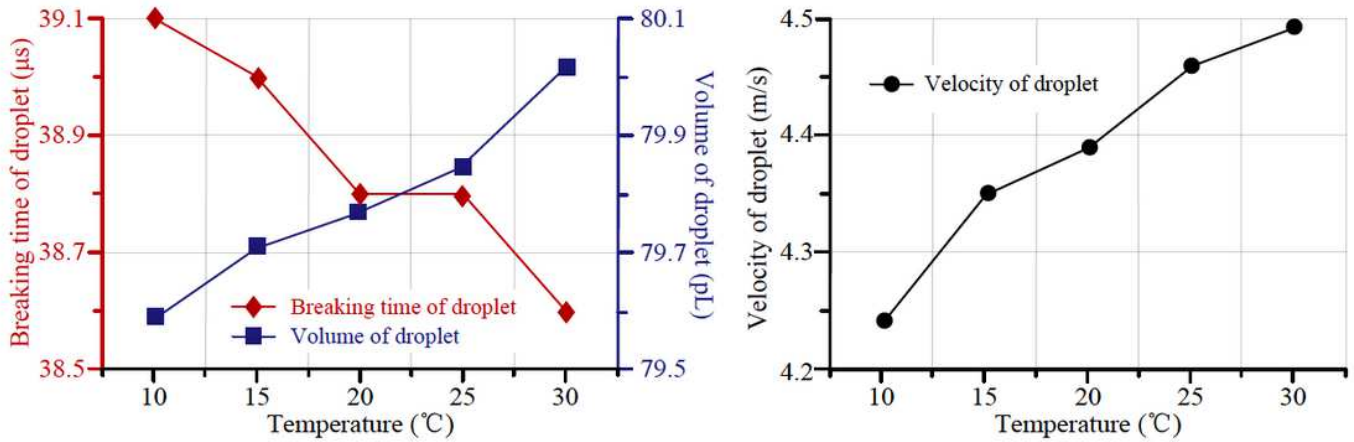

Figure 12

The relationship among breaking time of droplet, volume of droplet, velocity of droplet and liquid temperature

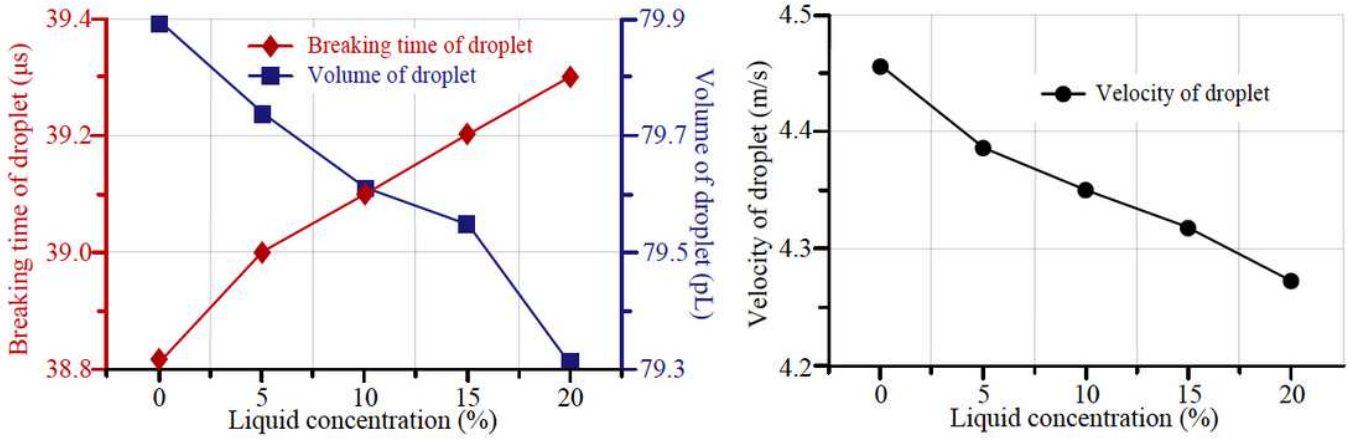

Figure 13

The relationship among breaking time of droplet, volume of droplet, velocity of droplet and liquid concentration

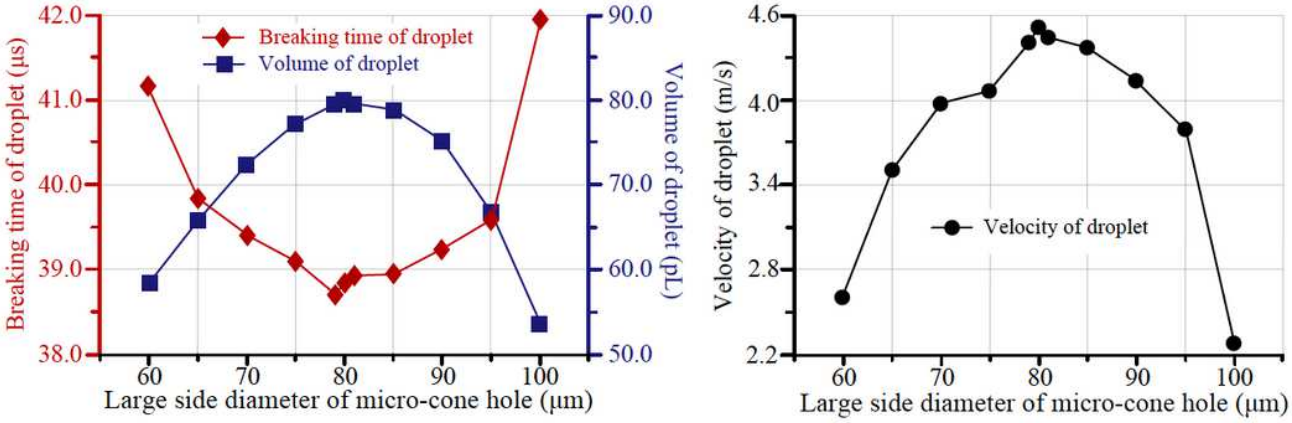

Figure 14

The relationship among breaking time of droplet, volume of droplet, velocity of droplet and large side diameter of micro-cone hole